

# Analysis and Design of a Wireless Closed-loop ICPT System Working at ZVS Mode

Rengui Lu, Tianyu Wang, Yinhua Mao, Chunbo Zhu

School of Electrical Engineering  
Harbin Institute of Technology  
Harbin, China  
lurengui@hit.edu.cn  
wangtianyu1985@hotmail.com  
myh1020@163.com  
zhuchubo@hit.edu.cn

**Abstract:** Based on the T-type equivalent circuit model of loosely coupled transformer, the theory of series-series (SS) resonant inductively coupled power transfer (ICPT) system was analyzed. By researching the principle of ICPT system working at zero voltage switch (ZVS) mode, the condition for realizing ZVS mode was got that the load resistance should be bigger than its critical value. According to the characteristic of open-loop ICPT system, a wireless voltage-feedback control for ICPT system working at ZVS mode was established. Based on the analysis above, An ICPT system prototype was built and tested, the maximum open-loop output power was 3.4KW, overall efficiency was 90%; the closed-loop output voltage was stable at 260V, and the maximum output power is 1.9KW.

**Keyword:** Inductively coupled power transfer (ICPT) , zero voltage switch(ZVS) , closed-loop

## I. INTRODUCTION

ICPT system can transfer energy from a power supply to a power consumer contactlessly basing on magnetic induction theory, the air gap between the power supply and the power consumer varies from several millimeters to centimeters. Such energy transfer has high security because of the non-contact feature, thereby ICPT systems have extensive application prospects, such as contactless charging systems for small electric cars [1], city electric public buses [2], AN Airborne radar [3], elevators [4] and autonomous underwater vehicle(AUV) [5].

Present researched ICPT systems are all open-loop [6-10], the closed-loop control method has not aroused attention yet; when the input voltage or the load fluctuates, system output voltage varies accordingly, hence a DC/DC converter should be added before load in order to output a stable voltage in practical applications, which of course will lead to a bigger volume and a higher cost of device.

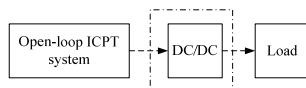


Figure 1. Open-loop ICPT system block diagram

As ICPT system's output power increases, how to make power converter work at ZVS mode becomes a key problem to be solved. In paper [11] a prototype with 3KW output power and 93% overall efficiency was built, which worked at zero current switch (ZCS) mode by adjusting working frequency according to primary peak current. Paper [12] introduced a method for realizing ZVS mode basing on Poincaré mapping and fixed points theory, but both systems mentioned above are open-loop, not closed-loop systems working at ZVS mode.

This paper researched the principle and condition for full-bridge phase-shift converter in series-series-resonant ICPT system working at ZVS mode, there was a critical value of load resistance related to the parameters of loosely coupled transformer and converter's phase-shifted angle. At certain phase-shifted angle, when the load resistance was bigger than the critical value, the full-bridge phase-shift converter of the ICPT system would be working at ZVS mode. Then a voltage-closed-loop controlling scheme was proposed, the parameters of discrete PI controller were determined according to the open-loop bode plot of the ICPT system. In this scheme, the secondary side outputted the voltage feedback signal which then was transmitted by RF module to the controller in the primary side; based on PI control algorithm, the controller outputted control parameter and adjusted the phase-shifted angle of full-bridge phase-shift converter accordingly to stabilize the output voltage of the secondary side. In the end, an ICPT system prototype with wireless voltage closed-loop control was built and tested, which worked at ZVS mode, the open-loop output power was 3.4kw, overall efficiency was 89%, and closed-loop output power was 2kw, stable output voltage was 260V.

## II. SS RESONANT THEORY

There are some basic traits for loosely coupled transformer, such as primary winding and secondary winding are fully separated, primary core and secondary core are also fully separated, and coupling coefficient is very low. As we know, to an ideal transformer(suppose turns ratio is 1:1), the no-load output voltage of secondary winding is just the same amplitude and phase as the voltage excitation in primary winding, while the same voltage excitation imposes on primary winding of a

loosely coupling transformer(suppose turns ratio is also 1:1), the no-load output voltage of secondary winding is smaller than the voltage of primary winding due to some fluxes generated by primary current is not through secondary winding. By the way, coupling coefficient or leakage inductance could be easily gotten by measuring primary voltage and self-inductance and the no-load voltage of secondary winding. Suppose turns ratio is 1:1, primary side and secondary side of loosely coupled transformer are symmetrical, thus primary self-inductance  $L_1$  is equal to secondary one  $L_2$ , so are the leakage inductances  $L_{1\delta}$  and  $L_{2\delta}$ (following analysis is all based on this suppose). The leakage inductance can be calculated by formula (1):

$$L_{1\delta} = \frac{V_{pri-pp} - V_{sec-pp}}{V_{pri-pp}} \times L_1 \quad (1)$$

Where  $V_{pri-pp}$  is the peak-to-peak voltage of high frequency excitation in primary side, and  $V_{sec-pp}$  is no-load peak-to-peak voltage of secondary coils.

In order to demonstrate the influence of leakage inductance on power transfer more easily, the T-type equivalent circuit model of loosely coupled transformer shown in Fig 2(a) is analyzed. Speaking simply, when the input excitation is high frequency (20k~100k), leakage inductive impedance may very big, even bigger than load impedance, which lead to the result that most of input energy distributes on leakage impedance while load impedance obtains very little, limiting the power transferred in system. In order to compensate the influence caused by leakage inductance, series-series resonant method is introduced: two series capacitors labeled as C1 and C2 are respectively added to both sides to make L1 and C1, L2 and C2 work in a resonant state, and they satisfy formulas (2) and (3),

$$C_1 = \frac{1}{\omega^2 \times L_{1\delta}} \quad (2)$$

$$C_2 = \frac{1}{\omega^2 \times L_{2\delta}} \quad (3)$$

Where  $\omega$  is the working angular frequency of the ICPT system. When the input of loosely coupled transformer is sinusoidal excitation with an angular frequency  $\omega$ , the simplified equivalent circuit for resonant tank which consists of compensation capacitors and loosely coupled transformer is shown in Fig 2(b), and the influence caused by leakage inductance can be compensated completely. But in practical application, the input is usually a square excitation with the same angular frequency, of which the duty ratio varies from 0%~100%, in this case, we can get Fourier series of the input square wave and analyze the ratio between fundamental wave' energy and the whole input energy, the bigger the ratio is, the better the compensation effect is.

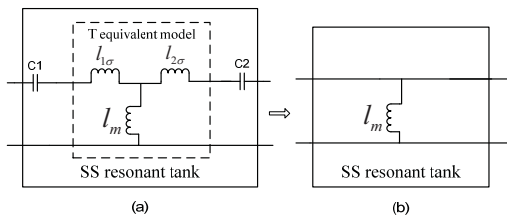


Figure 2. T-type equivalent circuit model of loosely coupled transformer & simplified circuit

### III. ANALYSIS OF ZVS MODE

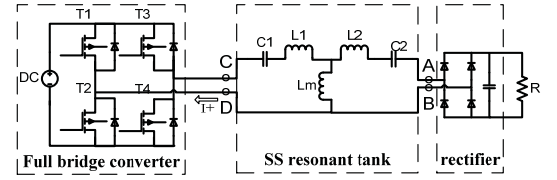


Figure 3. Main power circuit of SS resonant ICPT system

TABLE I. LOOSELY COUPLED TRANSFORMER'S PARAMETERS

Turn ratio	Air gap	Frequency f	Core cross-sectional area	
12:12	4mm	60k	26mm × 104mm	
$L_{1\sigma}$	$L_{2\sigma}$	$L_m$	C1	C2
35uh	34uh	65uh	205nf	210nf

The main power circuit of ICPT system is shown in Fig 3, the parameters of loosely coupled transformer, compensation capacitors and system working frequency are shown in Tab 1. The trigger signals for four MOSFET of full-bridge phase-shift converter are shown in Fig 4(a), MOSFET T1 and T2 are lagging legs, while MOSFET T3 and T4 are leading legs.  $\varphi$  denotes the phase-shift angle of full-bridge converter, and  $\varphi = T_\theta / T$  ( $T_\theta$  and T are marked in Fig 4(a)), its variation range is 0 ~ 180 degree. The output voltage waveform of full-bridge converter is shown in Fig 4(b), and the pulse width of output voltage is in proportion to phase shifting angle  $\varphi$ .

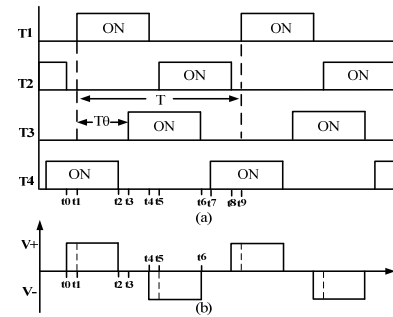


Figure 4. MOSFETs' trigger signals and converter's output voltage waveform

The path of system power flow is described as follow: full bridge converter changes the input DC voltage into square wave with an  $\omega$  angular frequency which acts as the excitation of resonant tank, then the output of resonant tank is rectified and filtered into DC voltage by diode detector and filtering capacitor for resistive load. As is analyzed in paper [1], when the input voltage and current of port AB (port AB is marked in Fig 3) are co-phasing and the filter afterwards is capacitive, the load resistance, rectifier and capacitive filter can be model by an equivalent resistor which can be calculated by formula (4):

$$R_{equ} = \frac{8}{\pi^2} \times R \quad (4)$$

So the circuit comprising SS resonant tank, rectifier, filter and load resistance  $R$  can be simplified as the circuit in Fig 5. For convenience, treat this circuit as the load of full-bridge phase-shift converter (in this chapter, the load mentioned afterwards means this circuit, not the load resistance  $R$ ).

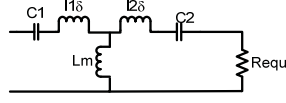


Figure 5. Equivalent circuit for SS resonant tank & rectifier & filter & load resistance  $R$

As shown in Fig 4, the whole working period  $t_0 \sim t_8$  of full-bridge phase-shift converter can be divided into 8 intervals. MOSFETs' on or off states are different in every interval. The following analysis will focus on converter's working states during the first half of period  $t_1 \sim t_5$ .

$t_1 \sim t_2$ : MOSFETs  $T_1$  and  $T_2$  turn on, full-bridge phase-shift converter infuses energy into resonant tank and the output voltage of converter is  $+V$  (take the potential of node C as reference ground). The ratio between this interval and the first half of period determines the power transferred. Fig 6(a) shows the current direction in full-bridge phase-shift converter at the time closer to  $t_2$ .

$t_2 \sim t_3$ : a dead time during which the up-leading leg  $T_3$  is off while the down-leading leg  $T_4$  is on, the output voltage of converter is 0. For the load circuit consists of energy storing components such as capacitor and inductor, the antiparallel diode of MOSFET  $T_3$  turns on and there is a freewheeling current in converter after MOSFET  $T_4$  turned off, the direction of this current is shown in Fig 6(b). At the time  $t_3$ , MOSFET  $T_3$  will be turned on by trigger signal at ZVS mode because there is a freewheeling current through antiparallel diode and the voltage drop of MOSFET  $T_3$  is close to 0.

$t_3 \sim t_4$ : MOSFETs  $T_1$  and  $T_2$  is on, converter's output voltage is 0, and energy storing components inside the load circuit are in zero-input-voltage state, the inductors' voltage and capacitors' current can be obtained by building and solving ordinary differential equations according to energy storing components' state at the time  $t_3$ , which is related to converter's phase-shift angle and dead time, the load resistance and loosely coupled transformer's parameters. The characteristic of load circuit's current is described from the views of experiment and simulation as follow: from the time  $t_3$ , the current through load circuit decreases gradually to zero then changes its direction, as the real current's curve in Fig 7 shows. According to energy storing components' different state at the time  $t_3$  and the time span of interval  $t_3 \sim t_4$ , there are two conditions at the time  $t_4$ : condition one, the current is still decreasing and its direction hasn't changed, as is shown in Fig 6(b); condition two, its direction has changed already, as is shown in Fig 6(e). These two conditions are corresponding respectively to converter's ZVS mode and hard-switching mode at the time  $t_5$ .

$t_4 \sim t_5$ : a dead time during which the up-lagging leg  $T_1$  is on while the down-lagging leg  $T_2$  is off.

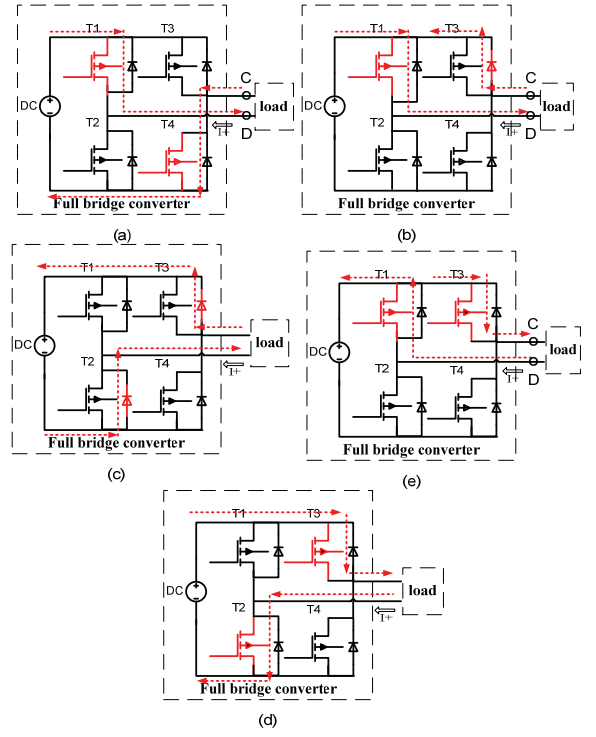


Figure 6. Current direction in the first half of period

Condition one: the current direction at the time  $t_4$  is shown in Fig 6(c). The antiparallel diode of MOSFET  $T_2$  is compelled to be on to provide a path for freewheeling current after MOSFET  $T_1$  turned off, then the output voltage of converter  $-V$  will make the freewheeling current decrease quickly. At the time  $t_5$ , if the freewheeling current still exists, MOSFET  $T_2$  will be turned on by trigger signal in ZVS mode. Compared to leading leg  $T_3$ , it's harder for lagging leg  $T_2$  to realize turning in ZVS mode (please refer to measured waveforms  $V_d$  and  $V_g$  of MOSFET  $T_2$  in Fig 7).

Condition two: the current direction at the time  $t_4$  is shown in Fig 6(e). When MOSFET  $T_2$  is turned on by trigger signal at the time  $t_5$ , the drain-source voltage of MOSFET  $T_2$  is  $+V$ . So MOSFET  $T_2$  is turned on in hard-switching mode (please refer to measured waveforms  $V_d$  and  $V_g$  of MOSFET  $T_2$  in Fig 7).

ZVS working principle of MOSFETs  $T_3$  and  $T_2$  in the first half of period is qualitatively analyzed above, analysis is the same for MOSFETs  $T_1$  and  $T_4$  in the second half of period.

Realizing lagging legs' ZVS mode is a key for whole converter's ZVS mode, and it can be affected by converter's phase-shift angle, dead time, and the system quality factor  $Q$ , which is defined by the following expression:

$$Q = \frac{|j\omega L_m|}{R} \quad (5)$$

When the system working phase-shift angle is  $120^\circ$  and dead time is  $1.5 \mu s$ , source voltage and drain-source voltage of MOSFET  $T_2$  and the output current of converter are tested at different load resistance, as is shown in Fig 7. From Fig 7 we can see, at the time  $t_5$ , the output current of converter is zero when the load resistance is  $30 \Omega$ ; the bigger the load

resistance is, the more margin for converter's output current to decrease, the drain-source voltage of MOSFET T2 is zero (please refer to  $V_{ds}$  waveform of MOSFET T2 when the load resistance is 100 Ohm in Fig 7), which belongs to ZVS mode; for the case that the load resistance is smaller than 30 Ohm, the output current of converter has already changed its direction at the time  $t_5$ , the voltage drop of MOSFET T2 is +V (please refer to  $V_{ds}$  waveform of MOSFET T2 when the load is 10 Ohm in Fig 7), which belongs to hard-switching mode. Thus 30 Ohm is the critical value of load resistance at this phase-shift angle, when the load resistance is bigger than 30 Ohm, converter would work at ZVS mode. Fig 8 shows the corresponding critical value of load resistance for phase-shift angle varying from  $180^\circ \sim 70^\circ$ .

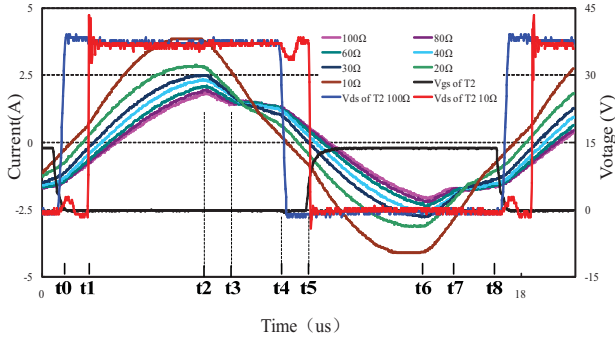


Figure 7. Critical value of load resistance testing chart when the phase-shift angle is  $120^\circ$

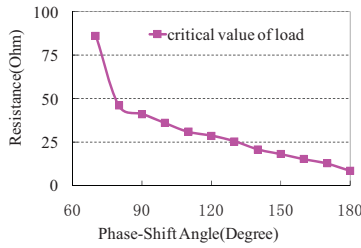


Figure 8. Critical values of load resistance for different phase-shift angle

Fix phase-shift angle at  $180^\circ$ , change load resistance from 20 Ohm to 100 Ohm (the critical value of load resistance is 13 Ohm when phase-shift angle is  $180^\circ$ ), test the output characteristic curve when DC input voltage is 290V, the results are shown in Fig 9 (the ambient temperature is  $12^\circ\text{C}$ ). The maximum output power can be 3400W, and system efficiency is above 90% when the output power is bigger than 1kw. The pictures of prototype are shown in Fig 10.

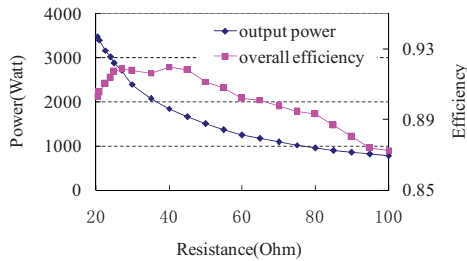


Figure 9. Output characteristic of open-loop ICPT system

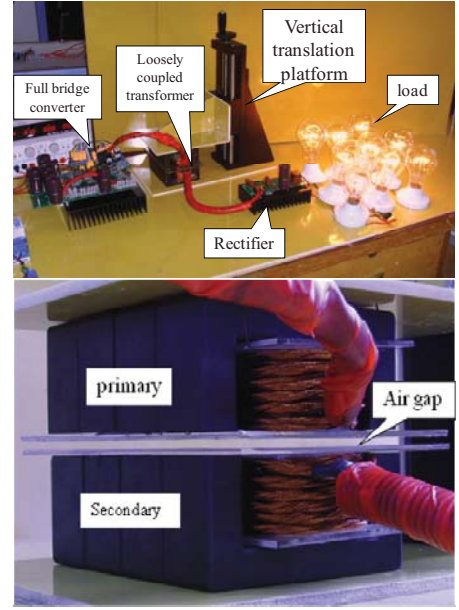


Figure 10. Open-loop ICPT prototype

#### IV. CLOSED-LOOP DESIGN OF THE ICPT SYSTEM

The objective of ICPT system' closed-loop controlling is to stabilize output voltage when the load varies or the input voltage fluctuates. The block diagram of closed-loop controlling system is shown in Fig 11, in which the process is resonant tank and load, actuator is full bridge converter. The controlling process is as follow: the voltage data of the load resistance is gathered by MCU and wirelessly transmitted by RF send module. The RF receive module in primary side gets the data and sends it to DSP controller, which will compares the data with the reference voltage, gets error signal and outputs control signal basing on PI control algorithm to adjust the phase shift angle of full-bridge phase-shift converter, equaling the output voltage to the reference voltage.

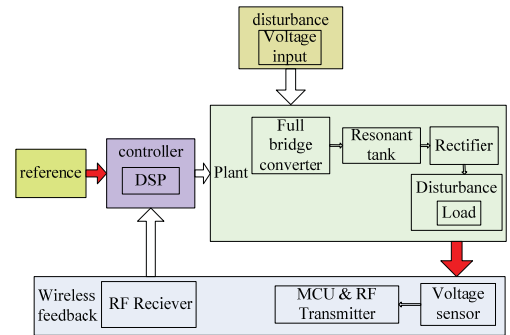


Figure 11. Closed-loop ICPT system block diagram

As Fig 8 shows, the critical value of load resistance is below 40 Ohm when the phase shift angle varies from  $180^\circ$  to  $100^\circ$ . Fix input voltage at 290V, and test the curves of output voltage changing with the phase shift angle when the load resistance is 100 Ohm and 40 Ohm. Results are shown in Fig 12.

Take output stable voltage is 260V as an example to design PI controlling parameters. From Fig 12 we can see, to output



260V, 40 Ohm load resistance corresponds to 140° phase shift angle while 100 Ohm load resistance corresponds to 120° phase shift angle. Thus take 130° phase shift angle as operation point, open-loop bode plot of the ICPT system is obtained as Fig 13 shows. By observing Fig 13, we can determine the gain value of closed-loop system to be -10db.

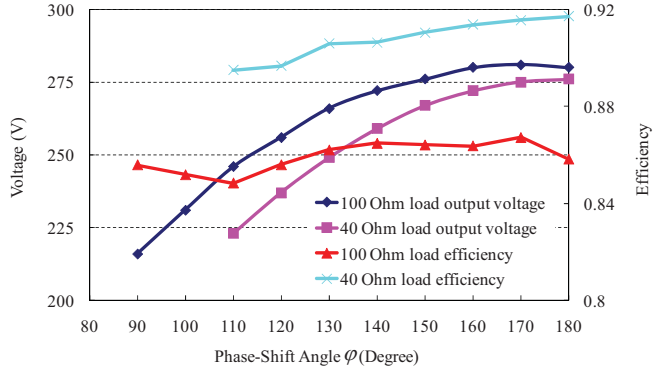


Figure 12. Efficiency and output voltage VS Phase-shift Angle

Considering that the changing frequency of load resistance is very low, setting the shearing frequency to be 30Hz can satisfy requirement of dynamic response. The analog PI controlling expressions are:

$$e(t) = V_{reference} - V_{feedback} \quad (6)$$

$$u(t) = 3.5e(t) + 659 \int e(t) \quad (7)$$

$$\varphi = \frac{180^\circ}{300} \times u(t) \quad (8)$$

Where  $V_{reference}$  is the reference voltage of the ICPT system,  $V_{feedback}$  is the load voltage,  $u(t)$  is the control variable and  $\varphi$  is converter's phase shift angle.

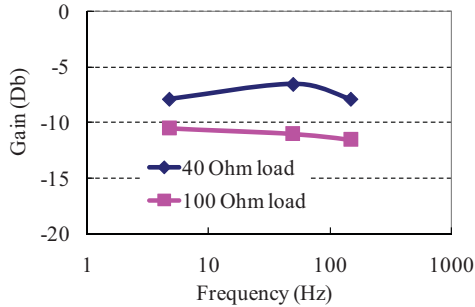


Figure 13. Amplitude frequency diagram

Discretize the three expressions above at a sample frequency of 300Hz, and complete phase-shift controlling process by TMS320F28335. Fig 14 shows the waveforms of system output current and voltage when the input voltage is 290V and the load resistance increases from 35 Ohm to 100 Ohm. The output voltage is stable at 260V, realizing the purpose of closed-loop control.

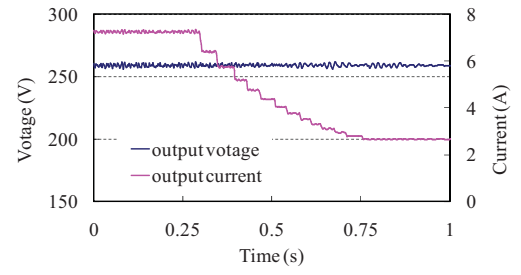


Figure 14. Closed-loop output characteristic when load resistance varies

## V. CONCLUSIONS

The critical value of load resistance for series-series resonant ICPT system which worked at ZVS mode was got by theoretic analysis and proved by experiments. An ICPT system which worked at ZVS mode was built and tested, at the air gap of 4mm, the maximum open-loop output power was 3.4KW and the overall efficiency was 98%. In order to stabilize the output voltage, a closed-loop voltage controlling system based on PI controlling algorithm was researched preliminarily. Experimental results showed that the output voltage can be stabilized when the load varied.

- [1] SAE Electric Vehicle Inductive Coupling Recommended Practice, SAE J-1773, Issued 1995-01, Revised 1999-11.
- [2] www.showa-aircraft.co.jp/products/EVkyuuden.html
- [3] K. D. Papastergiou, D. E. Macpherson, and F. Fisher, "An airborne radar power supply with contact-less transfer of energy—Part I: Rotating transformer," IEEE Trans. Ind. Electron., vol. 54, no. 5, pp. 2874–2884, Oct. 2007.
- [4] Ayan.H, Yamamoto.K, Hino.N, Yamato.I, "a highly efficient contactless electrical energy transmission system "IECON 02 ,2002 1364 – 1369.
- [5] Kojiya. T, Sato. F , Matsuki.H, Sato. T, " Automatic Power Supply System to Underwater Vehicles Utilizing Non-contacting Technology", OCEANS '04. MTS/IEEE TECHNO-OCEAN '04, 2341 – 2345.
- [6] J.T.Boys, G.A.Covic and A.W.Green. Stability and control of inductively coupled power transfer systems. IEE Proceedings: Electric Power Applications, v 147, n 1, p 37-43, Jan 2000
- [7] John T. Boys, Grant A. J. Elliott, Grant A. Covic, An Appropriate Magnetic Coupling Co-Efficient for the Design and Comparison of ICPT Pickups. IEEE Transactions on Power Electronics, v 22, n 1, p 333-335, January 2007
- [8] Nicholas A. Keeling, Grant A. Covic, John T. Boys A Unity-Power-Factor IPT Pickup for High-Power Applications. IEEE TRANSACTIONS ON INDUSTRIAL ELECTRONICS, February 2010 IEEE Transactions on Industrial Electronics, v 57, n 2, p 744-751,
- [9] A. Ecklebe and A. Lindemann Analysis and design of a contactless energy transmission system with flexible inductor positioning for automated guided vehicles IECON Proceedings (Industrial Electronics Conference), 2006, p 1721-1726,
- [10] Moradewicz, Artur ,Kazmierkowski, Marian P. FPGA Based Control of Series Resonant Converter for Contactless Power Supply, IEEE International Symposium on Industrial Electronics, p 245-250, 2008
- [11] A.J. MORADEWICZ and M.P. KAZMIERKOWSKI High efficiency contactless energy transfer system with power electronic resonant converter BULLETIN OF THE POLISH ACADEMY OF SCIENCES TECHNICAL SCIENCES Vol. 57, No. 4, 2009.
- [12] Chun Sen Tang, Yue Sun, Yu Gang Su, Sing Kiong Nguang, Aiguo Patrick Hu, "Determining Multiple Steady-State ZCS Operating Points of a Switch-Mode Contactless Power Transfer System", IEEE TRANSACTIONS ON POWER ELECTRONICS, VOL. 24, 2009